The Influence of shearing and rotary inertia on the resonant properties of gold nanowires

Pär A. T. Olsson,[1,a)] Harold S. Park,[2] and Per C. Lidström[1]
[1]*Division of Mechanics, Lund University, P.O. Box 118, SE-221 00 Lund, Sweden*
[2]*Department of Mechanical Engineering, Boston University, Boston, Massachusetts 02215, USA*

(Received 20 July 2010; accepted 2 October 2010; published online 23 November 2010)

In a previous publication [P. A. T. Olsson, J. Appl. Phys. **108**, 034318 (2010)], molecular dynamics (MD) simulations have been performed to study the resonant properties of gold nanowires. It has been documented in the aforementioned publication that the eigenfrequencies of the fundamental mode follows the continuum mechanically predicted behavior when Bernoulli–Euler beam theory is used, whereas the higher order modes tend to be low in comparison to Bernoulli–Euler beam theory predictions. In this work, we have studied the resonant properties of unstressed and prestressed nanowires to explain why the eigenfrequencies of the fundamental mode follows the behavior predicted by Bernoulli–Euler beam theory while those of higher order modes are low in comparison. This is done by employing Timoshenko beam theory and studying the nanowire deformations for different modes. We find good agreement between the MD results and Timoshenko predictions due to the increasing importance of shearing and rotary inertia for higher order resonant modes. Furthermore, we argue that this type of behavior is merely a geometric effect stemming from low aspect ratio for the considered structures as a converging type of behavior is found when the aspect ratios fall between 15 and 20. Finally, we have found that classical Timoshenko beam theory that neglects nanoscale surface effects is able to, simply through utilization of the size dependent Young's modulus, capture the dynamic properties of the gold nanowires as calculated through MD.
 [doi:10.1063/1.3510584]

I. INTRODUCTION

Over the past decade, extensive research efforts have been invested in trying to understand the mechanical properties of nanowires. One of the major reasons behind this immense interest is the fact that the nanowire constitutes one of the potential structural elements in nanoelectromechanical systems (NEMS). Due to their small dimensions, spanning from hundreds down to only a few nanometers, nanowires tend to exhibit many remarkable physical properties such as high force sensitivity, low mass, and a high eigenfrequency spectra which allows nanowires to naturally operate in the megahertz and gigahertz regimes. Consequently, this makes nanowires ideal candidates to be employed in various sensing applications such as measurements of molecular interactions and mass detection where the sensing is performed by monitoring shifts in the natural frequency spectrum.[1–4]

To predict the correct frequency shifts it is essential that the continuum mechanical models accurately describe the elastic properties of the structure. However, nanosized structures are known to have physical properties which are quite different from that of macroscopic bodies, which comes from the fact that the fraction of surface atoms is negligible for macroscopic structures, whereas for nanosized structures it is very large. Since surface atoms have lower coordination (i.e., fewer bonding neighbors) than bulk atoms, they tend to display quite different mechanical properties from their bulk counterparts. Consequently, the surface properties become increasingly important at the nanoscale, and dictate the overall mechanical behavior of nanostructures.[5,6] This becomes particularly important when nanowires are subjected to transverse loading because the top and bottom surfaces are subject to the greatest amounts of tensile or compressive stress as the nanowires are deformed. Hence, given the different physical properties of surfaces one might expect an enhanced surface influence, and, therefore, also differences in the Young's moduli of nanowires that are obtained from bending or transverse vibrational spectra as compared to those obtained from tensile experiments or simulations.[7–9]

Experimentally, elastic properties of nanowires are normally determined either through dynamic resonance experiments[1–4,10–19] or through bending experiments[20–26] where the elastic properties are determined from continuum mechanical relations connecting the deflection or resonance properties with the Young's modulus. However, there are issues which complicate the investigation severely that are typically not taken into account. One such issue is whether or not there are any axial stresses present.[16] This is a quite critical problem as axial stresses will influence the eigenfrequency spectrum as well as the static deflection and may lead to erroneous results when obtaining the size dependent Young's modulus. Axial stresses can also be quite useful as it opens up the possibility to manufacture resonators with variable eigenfrequency spectra, where the natural frequencies are controlled by varying the applied axial strain. This has become particularly relevant for NEMS-based sensing applications where high quality factors of the nanoresonators is essential for enhanced sensing capabilities.[17–19]

Numerically, Park performed finite element simulations

a)Electronic mail: par.olsson@mek.lth.se.

with the surface Cauchy–Born[27,28] (SCB) and bulk Cauchy–Born models to study how axial strains resulting from surface stresses influence the fundamental eigenfrequency. It was found, in agreement with analytical models,[29,30] that the introduction of surface stresses lead to a higher or lower fundamental eigenfrequency if the nanowires are prevented to relax axially. This is due to the character of the surface stress, which can be either compressive (for silicon) or tensile (for fcc metals).[31–33] In addition to finite element calculations, molecular dynamics (MD) simulations have been performed to study bending properties and eigenfrequency spectra of nanowires.[9,34–37] Broughton *et al.*[34] performed MD simulations to study how well the eigenfrequency spectrum of quartz oscillators corresponds to that of Bernoulli–Euler continuum beam theory. Interestingly, they found that due to nanoscale surface effects, the eigenfrequencies from the MD simulations to be consistently low in comparison to Bernoulli–Euler continuum beam theory. Cao *et al.* studied how the fundamental eigenfrequency of carbon nanotubes behaves under different amounts of tensile and compressive strains, and found good agreement between Bernoulli–Euler continuum beam theory and the MD results.[35] Olsson studied how well the three lowest eigenfrequencies of strained gold nanowires agreed with what was predicted from Bernoulli–Euler continuum beam theory and found a remarkably good agreement between MD results and the continuum predictions for the fundamental mode when the size dependent Young's moduli were used. The higher order modes, however, were found to be consistently lower than the predictions from continuum beam theory.[36]

The objective of this paper is therefore to explain why the eigenfrequencies of excited modes obtained in previous works[34,36] are low in comparison Bernoulli–Euler beam theory. This is done by employing a higher order beam theory and by studying the details of nanowire deformation through MD simulations.

II. CONTINUUM BEAM THEORY

A. Bernoulli–Euler

The differential equation governing free plane transverse vibrations of an axially homogeneous prestressed Bernoulli–Euler beam can be written as

$$EI\frac{d^4w}{dx^4} - \sigma A\frac{d^2w}{dx^2} - \omega^2\rho A w = 0, \tag{1}$$

where σ, E, I, ω, w, ρ, and A denote the applied axial stress, Young's modulus, moment of inertia, angular frequency, deflection of the center line, volume specific mass density, and the cross sectional area, respectively. The frequency is related to the angular frequency through $f=\omega/2\pi$.[38] The secular equation from which the eigenfrequencies of a biclamped beam can be calculated has been derived in Ref. 39.

B. Timoshenko

In the basic kinematic assumptions for Bernoulli–Euler beam theory it is assumed that shearing and rotary inertia can be neglected. To account for these quantities we resort to Timoshenko beam theory which takes both into account. This means that the cross sections are not assumed to be orthogonal to the center line of the beam and that the effective mass of the system increases. Hence, to go from Timoshenko beam theory to Bernoulli–Euler beam theory, one needs to impose a scleronomic constraint and reduce the effective mass, which means that Bernoulli–Euler beam theory has lower effective mass and is stiffer than that of Timoshenko. Thus, the eigenfrequencies of Timoshenko beam theory, in general, are lower than those of Bernoulli–Euler beam theory.[38,40]

The differential equations governing free transverse vibrations of a prestressed Timoshenko beam can be written as[41]

$$(\sigma A + k_s GA)\frac{d^2w}{dx^2} - k_s GA\frac{d\psi}{dx} + \omega^2\rho A w = 0, \tag{2}$$

$$I(\sigma + E)\frac{d^2\psi}{dx^2} + k_s GA\left(\frac{dw}{dx} - \psi\right) + \omega^2\rho A r^2\psi = 0, \tag{3}$$

where ψ is the rotation of the cross section and k_s and G denote the cross sectional reduction factor and the shear modulus, respectively. The quantity $r=\sqrt{(I/A)}$ is the radius of gyration and is related to the rotary inertia and the factor k_s is approximately 5/6 for rectangular and square cross sections. If it is assumed that the rotary inertia is small and the stress is small compared to Young's modulus, i.e., $r\to 0$ and $\sigma+E\approx E$, then in the limit of $G\to\infty$ the shearing becomes negligible which ensures that Eqs. (2) and (3) simplify to Eq. (1). With the boundary conditions for a biclamped Timoshenko beam, given by $\psi=w=0$ at the end points, it is possible to derive the secular equation from which the eigenfrequencies can be calculated.

III. MD SIMULATIONS

We considered defect-free single crystal gold nanowires with square cross sections and with a ⟨100⟩ crystallographic orientation with {100} transverse side surfaces. Three different nanowire sizes have been simulated; 4.08×4.08 nm^2, 5.71×5.71 nm^2, and 7.34×7.34 nm^2 cross sectional sizes, with the respective unrelaxed lengths 49.0 nm, 68.5 nm, and 88.1 nm. These samples have aspect ratios which are roughly 12. In addition, for the 4.08×4.08 nm^2 nanowires we have also varied the length to study how the eigenfrequency spectrum was influenced by the aspect ratio, where the studied aspect ratios ranged from about 8 to 17.

The simulations were performed at two different temperatures; liquid helium and room temperature, i.e., 4.2 K and 300 K, respectively. Results from two types of MD simulations have been studied; mixed mode and pure mode simulations. Mixed mode simulations were performed to obtain the three lowest eigenfrequencies, while the pure mode simulations were performed so that the deformations of the pure modes can be obtained which will enable us to delineate the magnitudes of the shearing for the different modes. The interatomic interactions were modeled through an embedded atom method (EAM) potential for gold given in Ref. 39. This potential describes the elastic properties very well which is

of great importance for this application as we are interested in describing the mechanical properties accurately.

The atoms were initially placed according to a perfect fcc lattice and then homogeneously strained in the direction of the wire axis so that the interplanar distance corresponds to that of the desired strain state. The reference configuration was chosen to be the state where the resulting axial stress is zero for the appropriate size and temperature. This means that the ideal interplanar distance along the wire axis does not correspond to the zero strain state. To mimic biclamped conditions we let the atoms of the three outermost fcc cells closest to the ends be fixed throughout the simulation. To study the dynamic response, we follow the numerical strategy from Ref. 36, where the nanowires are first subjected to an external load, Q, in one of the lateral directions. Then the static state of equilibrium is found using an energy minimization algorithm, whereafter the nanowire is equilibrated to the target temperature using a thermostat with the load still acting on the nanowire. Once the nanowire is equilibrated the load is released and the free atoms are set to follow the microcanonical equations of motion. To obtain the dynamic response we divided the nanowire into discrete masses which were obtained by dividing the wire into equally sized segments along the wire axis. The centers of gravity for these discrete masses were then monitored throughout the simulation. To extract the eigenfrequencies of the system, the dynamic history of the masses were then Fourier transformed. For the mixed mode simulations the external load, Q, was distributed over half the wire length. The only difference when studying pure modes was that different load distributions, Q, were used to excite as pure modes as possible. The process for obtaining these load distributions was a trial and error procedure and the load distributions that we finally ended up using for the pure mode simulations were the following:

$$Q_1 = q \quad 0 < x \leq L, \tag{4}$$

$$Q_2 = \begin{cases} q & 0 < x \leq L/2 \\ -q & L/2 < x \leq L \end{cases}, \tag{5}$$

$$Q_3 = \begin{cases} q & 0 < x \leq 3L/8 \\ -q & 3L/8 < x \leq 5L/8 \\ q & 5L/8 < x \leq L \end{cases}, \tag{6}$$

for the three lowest modes, respectively, where q denotes the magnitude of the load and x is the coordinate along the wire axis. Some of the MD results used here for comparison for the mixed mode strategy have already been published previously.[36]

IV. RESULTS AND DISCUSSION

When comparing the MD results with the Timoshenko and Bernoulli–Euler continuum models it is assumed that the stress follows a cubic polynomial of the strain, thus we assume the stress can be written as

TABLE I. Quantities of the polynomial in Eq. (7) that describe the nonlinear size dependent elastic properties of the considered nanowires.

	T (K)	E (GPa)	C_2 (GPa)	C_3 (GPa)
4.08×4.08 nm^2	4.2	39.0	379	−2440
	300	33.8	391	−5280
5.71×5.71 nm^2	4.2	41.6	361	−2380
	300	39.1	342	−4260
7.34×7.34 nm^2	4.2	42.9	360	−2490
	300	41.8	351	−6150

$$\sigma = E\epsilon + \frac{1}{2}C_2\epsilon^2 + \frac{1}{6}C_3\epsilon^3, \tag{7}$$

where E denotes Young's modulus and the constants C_2 and C_3 are nonlinear contributions. We do emphasize that this relation is used only to approximate the axial stress in Eqs. (1)–(3) for a given size and strain. The choice of a cubic polynomial was made out of convenience as it described the stress versus strain curves very accurately. To obtain values which capture the size and strain dependencies, we fitted the polynomials to previously published size dependent stress vs. strain curves for the used EAM potential.[36] The resulting quantities can be seen in Table I, from which it can be observed that the stiffness (E) decreases with decreasing size for the current crystallographic orientation. The corresponding bulk values of Young's moduli were found to be 46.1 GPa and 42.4 GPa at 4.2 K and 300 K, respectively. When approximating the shear modulus used for the Timoshenko calculations it is assumed that the shear modulus corresponds to the value of C_{44}=45.4 GPa which the potential was fitted to. This is of course an approximation as, in analogy to the stiffness, we might expect that there is a variation due to size dependence, temperature and strain due to surface-stress-induced lattice contractions.

A. Mixed modes

In Table II, we have collected the resulting eigenfrequencies of unstressed nanowires along with results from analytical continuum mechanical calculations, where the Young's modulus that is necessary for the analytical calculations were obtained from the MD simulations in Table I. For some of the entries there is a range of values; the reason for this is that many simulations were performed with different load magnitudes and thus there are small nonlinear contributions influencing the eigenfrequencies. However, the variations are only of the order of a few percent. Comparing the eigenfrequencies of the fundamental mode with the results from the MD simulations it can be seen that the overall agreements are good. For the low temperature simulations it is found that the fundamental eigenfrequency calculated using Timoshenko beam theory is almost in perfect agreement with the MD results. This is also the case for the 4.08×4.08 nm^2 nanowire at 300 K, but not for the 5.71×5.71 nm^2 and 7.34×7.34 nm^2 nanowires at room temperature. For the fundamental mode, the deviations between Timoshenko and Bernoulli–Euler beam theory results and those of MD are

TABLE II. The three lowest eigenfrequencies f_1, f_2, and f_3 for the unstressed nanowires. MD are results from MD simulations, A_{B-E} are results from Bernoulli–Euler continuum mechanical calculations and A_T are results from Timoshenko continuum mechanical calculations. The MD results are taken from Ref. 36.

	T (K)		f_1 (GHz)	f_2 (GHz)	f_3 (GHz)
4.08×4.08 nm^2	4.2	MD	2.71–2.78	7.28–7.33	13.8–13.9
		A_{B-E}	2.83	7.81	15.3
		A_T	2.78	7.43	14.0
	300	MD	2.56–2.63	6.87–6.95	12.9–13.2
		A_{B-E}	2.64	7.27	14.3
		A_T	2.59	6.96	13.2
5.71×5.71 nm^2	4.2	MD	1.95–1.97	5.24–5.25	9.92–9.94
		A_{B-E}	2.01	5.55	10.9
		A_T	1.97	5.28	9.97
	300	MD	1.99	5.19–5.20	9.62–9.87
		A_{B-E}	1.94	5.35	10.5
		A_T	1.90	5.10	9.65
7.34×7.34 nm^2	4.2	MD	1.53	4.09	7.74
		A_{B-E}	1.56	4.29	8.41
		A_T	1.52	4.08	7.71
	300	MD	1.54–1.55	4.05–4.19	7.50
		A_{B-E}	1.53	4.22	8.27
		A_T	1.50	4.02	7.60

less than 5% so both Bernoulli–Euler and Timoshenko beam theories can be considered to reproduce the MD results quite accurately. For the first and second excited modes it is found that the results from Timoshenko beam theory are in better agreement with the MD results, whereas Bernoulli–Euler beam theory displays consistently higher eigenfrequencies than what was obtained from MD simulations.

Bernoulli–Euler beam theory predicts certain ratios between the three lowest unstressed eigenfrequencies $R_{31}=f_3/f_1=5.40$, $R_{32}=f_3/f_2=1.96$, and $R_{21}=f_2/f_1=2.76$. These ratios are independent of the stiffness and geometry when Bernoulli–Euler beam theory is used. The same ratios obtained from MD simulations fall in the following intervals; $4.83<R_{31}<5.14$, $1.79<R_{32}<1.91$, and $2.61<R_{21}<2.70$. When comparing these ratios it is clear that the ratios predicted from Bernoulli–Euler beam theory act as upper bounds for the MD results. For the considered samples we find that the same ratios predicted from Timoshenko theory are slightly lower than those from Bernoulli–Euler beam theory, $5.04<R_{31}<5.10$, $1.89<R_{32}<1.90$, and $2.62<R_{21}<2.69$. These intervals fall within the bounds that were obtained from MD simulations, and the agreement does, therefore, appear to be improved by the utilization of Timoshenko beam theory rather than Bernoulli–Euler theory.

In Table III, we have analytically studied what happens if the rotary inertia is neglected ($r\to0$), if there is no shearing ($G\to\infty$) or both, and compared the findings with results from MD and analytical Timoshenko calculations. The considered sample is an unstressed 4.08×4.08 nm^2 nanowire at 300 K. Comparing with the results in Table II, it is seen that if both the rotary inertia and the shearing are neglected, we get the same results as if we solve the Bernoulli–Euler secular equation for an unstressed nanowire. It is also found that neglecting shearing leads to higher eigenfrequencies than neglect of rotary inertia does. This finding may not be a general observation as it probably depends on material and crystallographic orientation, but it applies for this particular case. Furthermore, it implies that the neglect of shearing is more important than the neglect of rotary inertia when explaining the discrepancies between Bernoulli–Euler results and MD results. Nevertheless, both quantities appear to be important when it comes to predict the eigenfrequency spectrum accurately.

In Fig. 1, we have compared the fundamental eigenfrequency from MD simulations with that calculated from the secular equations of biclamped Bernoulli–Euler and Timoshenko beams. Equation (7) was used when calculating how the stress varies with strain. The strain is measured from the relaxed state so that the resulting axial force is zero when the

TABLE III. The three lowest frequencies for an unstressed 4.08×4.08 nm^2 nanowire under the assumptions of neglected rotary inertia ($r\to0$) and/or shearing ($G\to\infty$). MD are results from MD simulations and A_T are results from Timoshenko continuum mechanical calculations.

	MD	A_T	$r\to0$	$G\to\infty$	$r\to0$, $G\to\infty$
f_1 (GHz)	2.56–2.63	2.59	2.60	2.63	2.64
f_2 (GHz)	6.87–6.95	6.96	7.05	7.16	7.27
f_3 (GHz)	12.9–13.2	13.2	13.5	13.8	14.3

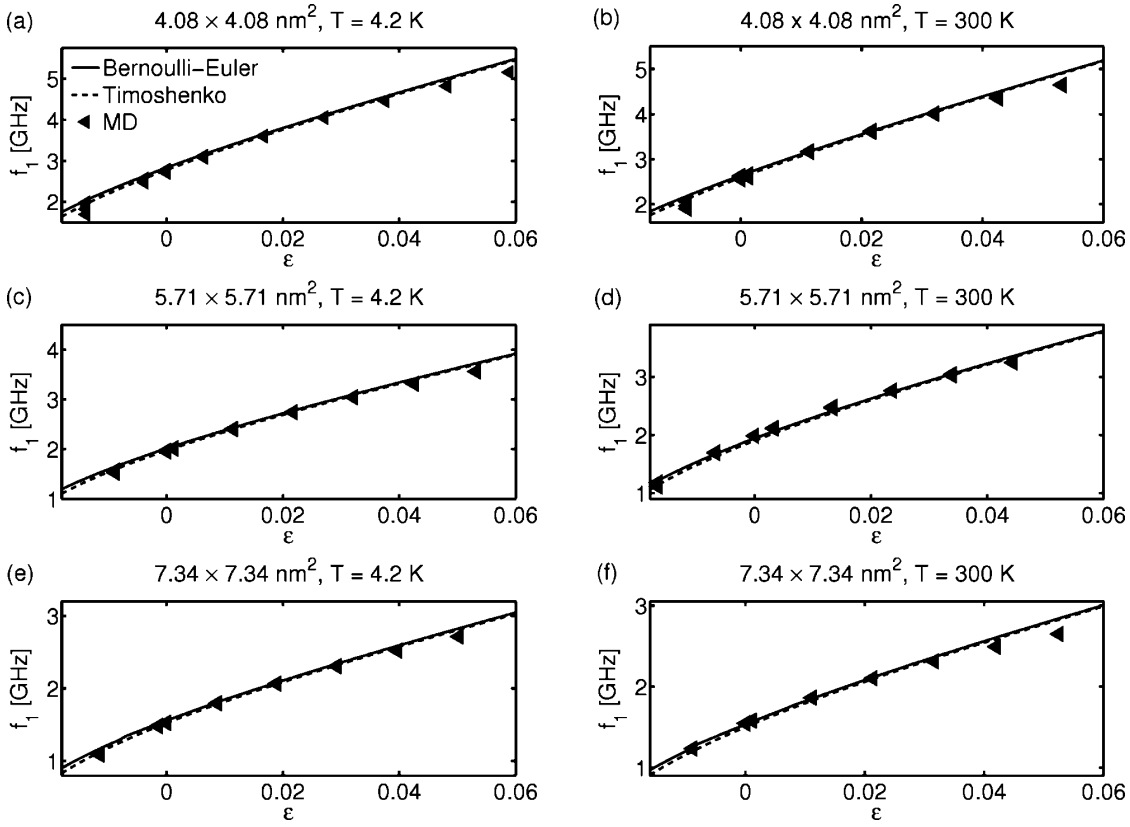

FIG. 1. Eigenfrequencies of the fundamental mode (f_1) for different amounts of strain for 4.08×4.08 nm^2 sized nanowires at (a) 4.2 K and (b) 300 K, 5.71×5.71 nm^2 sized nanowires at (c) 4.2 K and (d) 300 K, and 7.34×7.34 nm^2 sized nanowires at (e) 4.2 K and (f) 300 K. The MD results are taken from Ref. 36.

strain is zero and the interplanar distance between the vertical atomic planes does not correspond to that of an ideal lattice. It can be seen that the overall agreement between MD, Timoshenko, and Bernoulli–Euler beam theory is good, particularly, when the magnitudes of the strain are small. However, at larger strains, it is found that both the Bernoulli–Euler and Timoshenko beam theories are somewhat stiff in comparison with MD results. This is likely due to the fact that the higher order contributions in terms of stresses have been neglected in Eqs. (1)–(3). Obviously these contributions become increasingly important with increasing strain.

In previous investigations, analytical calculations[29,30] and SCB calculations[31,32] have been used to study the influence of strain on the eigenfrequency spectrum and static deflection of nanowires subjected to tensile surface stresses. It has been observed that the eigenfrequencies increase and the static deflection decrease when surface stresses are present, which implies an increased stiffness. But that depends on how the strains are measured. In this work, the strains are measured from the unstressed state, whereas in previous works[29–32] the strains are measured from the perfect lattice constant. When the strains are measured from the perfect lattice constant the resulting axial stress is not zero when surfaces are introduced, and this contributes to a higher eigenfrequency spectrum than what would be obtained if the nanowires were stress-free. Hence, the results in this paper reveal the same trends as the results of previous works.

The strain dependence on the eigenfrequencies of the first excited mode has been studied in Fig. 2. What becomes immediately clear by investigation is that there is an increasing discrepancy between the Bernoulli–Euler and Timoshenko continuum predictions compared to the fundamental mode as the eigenfrequencies from Timoshenko theory are low in comparison with those from Bernoulli–Euler beam theory. The eigenfrequency spectrum obtained from MD simulations at low temperature appears to be in very good agreement with the Timoshenko results. For the room temperature simulations it is found that there is a good agreement between MD and Timoshenko results when the strains are small. At strains around 2% the MD results fall essentially between the Timoshenko and Bernoulli–Euler predictions. At even higher strains we find that both the continuum models slightly overestimate the eigenfrequencies obtained from MD, in the same manner as for the fundamental mode. Again, this is likely due to the neglect of higher order contributions in terms of stresses in Eqs. (1)–(3).

In Fig. 3, we have studied the influence of strain on the second excited mode. It can be observed that the relative discrepancy between the Bernoulli–Euler and Timoshenko solutions has increased in comparison to the fundamental and first excited modes. Furthermore, it appears that the MD results follow the Timoshenko solutions quite closely and that the Bernoulli–Euler solutions are stiff in comparison.

Based on Figs. 1–3, it appears as if the Timoshenko predictions are in better agreement with the MD results when higher modes are considered. This is an indication that the higher modes are subjected greater amounts of shearing and that the contribution of the rotary inertia to the kinetic energy

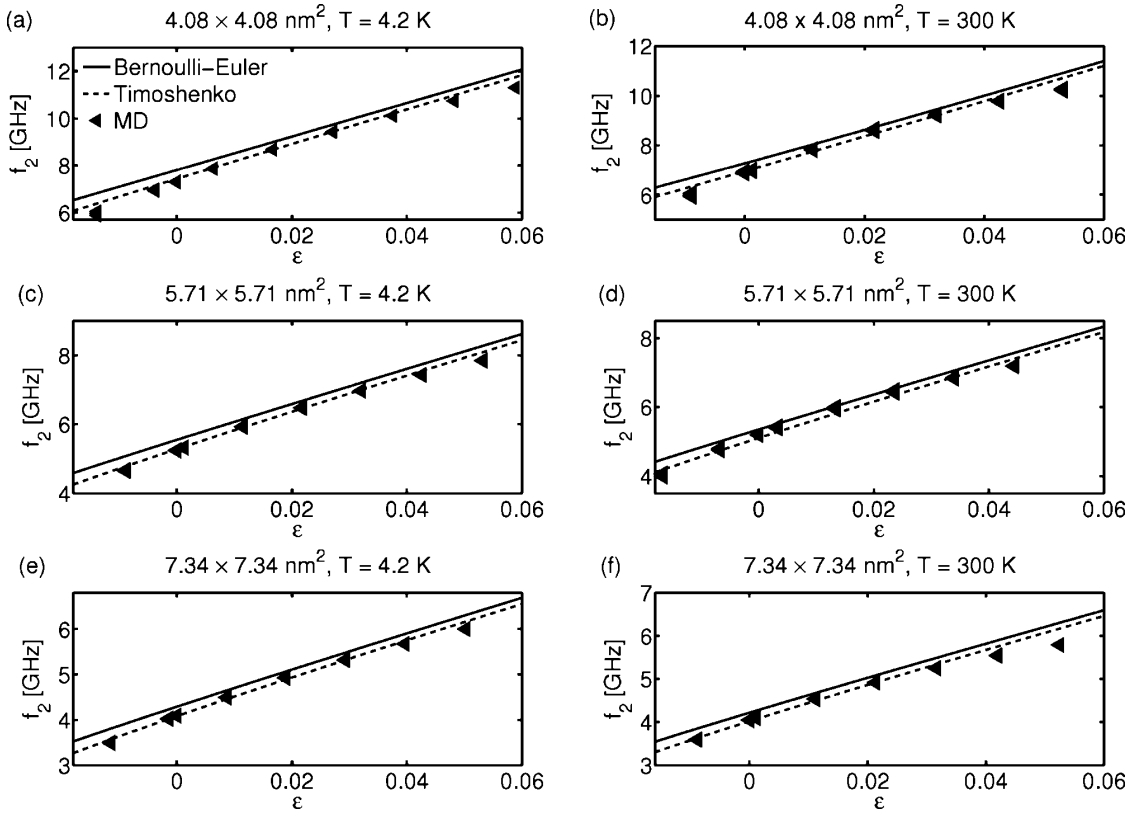

FIG. 2. Eigenfrequencies of the first excited mode (f_2) for different amounts of strain for 4.08×4.08 nm^2 sized nanowires at (a) 4.2 K and (b) 300 K, 5.71×5.71 nm^2 sized nanowires at (c) 4.2 K and (d) 300 K, and 7.34×7.34 nm^2 sized nanowires at (e) 4.2 K and (f) 300 K. The MD results are taken from Ref. 36.

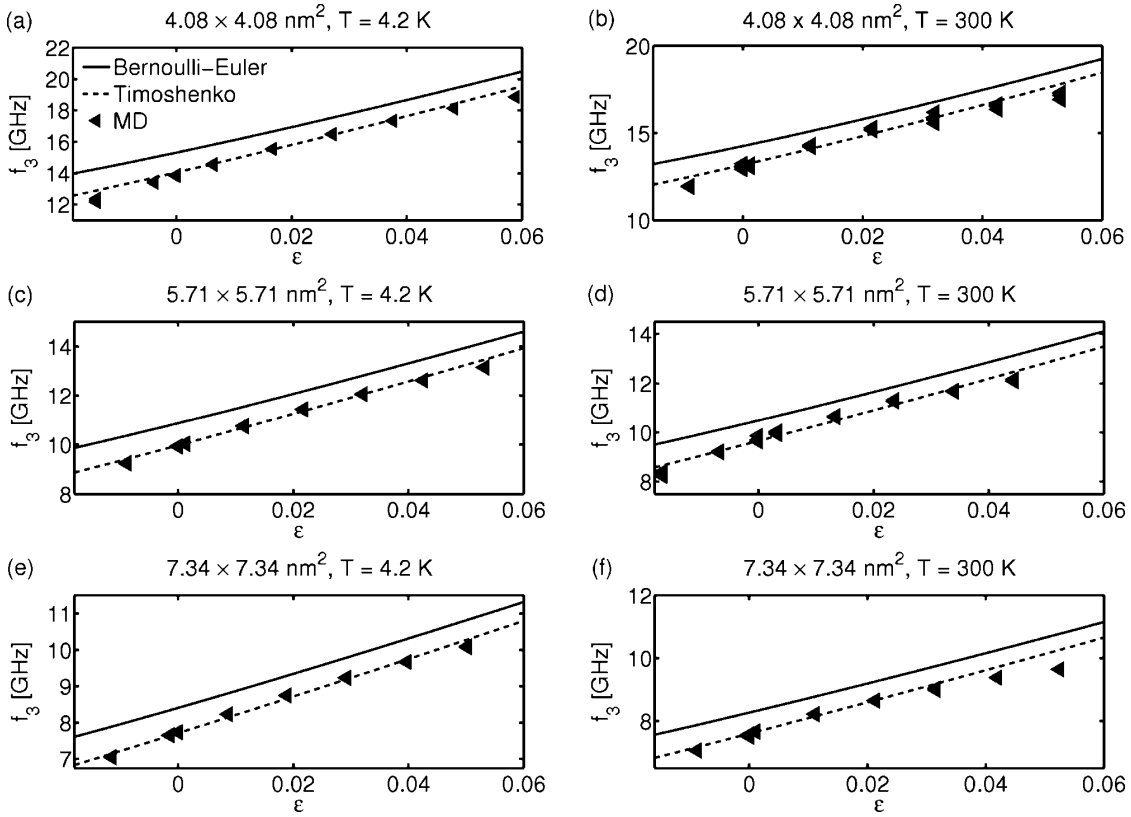

FIG. 3. Eigenfrequencies of the second excited mode (f_3) for different amounts of strain for 4.08×4.08 nm^2 sized nanowires at (a) 4.2 K and (b) 300 K, 5.71×5.71 nm^2 sized nanowires at (c) 4.2 K and (d) 300 K, and 7.34×7.34 nm^2 sized nanowires at (e) 4.2 K and (f) 300 K. The MD results are taken from Ref. 36.

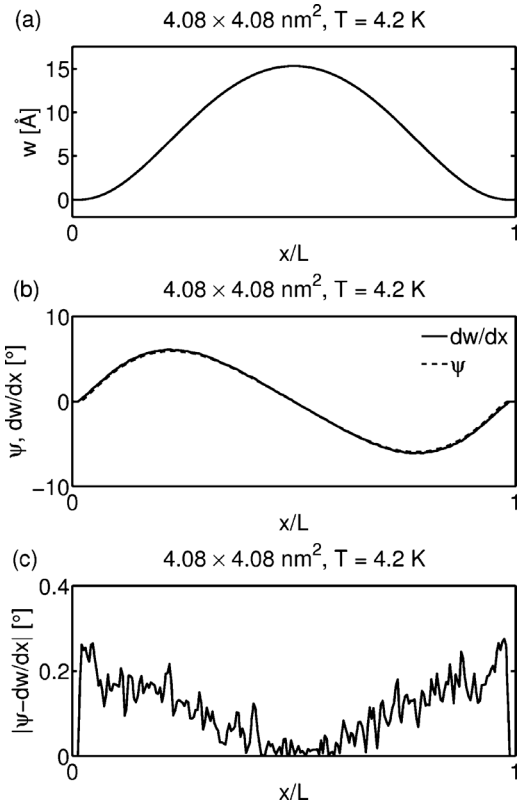

FIG. 4. Snapshot of the nanowire when the fundamental mode is the dominating exciting mode. (a) Deflective shape of the center line for the snapshot, (b) the deflective angle of the center line and the rotation angle of the vertical atomic planes, and (c) the difference between the deflective angle and the rotation angle.

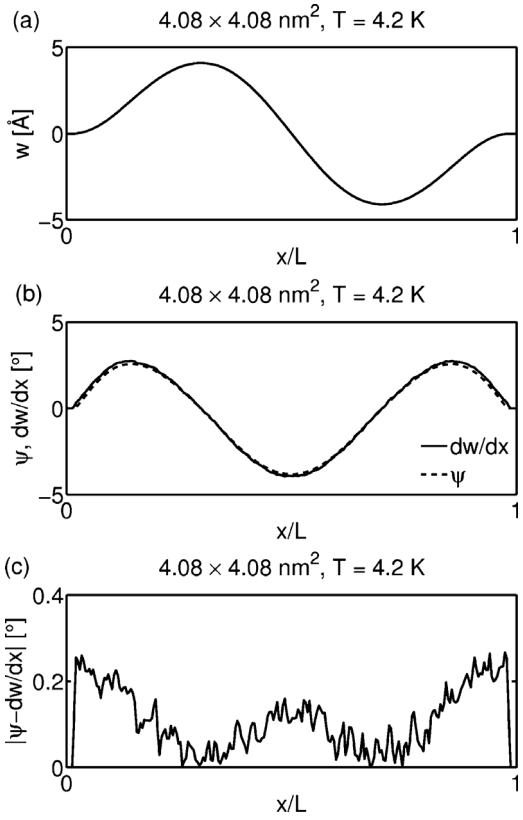

FIG. 5. Snapshot of the nanowire when the first excited mode is the dominating exciting mode. (a) Deflective shape of the center line for the snapshot, (b) the deflective angle of the center line and the rotation angle of the vertical atomic planes, and (c) the difference between the deflective angle and the rotation angle.

becomes increasingly important, which makes sense as the number of inflection points of the mode shape as well as the eigenfrequency increase with higher modes.

However, what is more interesting is that, even for the very small nanowires (<10 nm cross sections) that we have studied, we are able to obtain an extremely good agreement between the MD results and the theoretical Timoshenko theory using only the appropriate size dependent Young's modulus. In fact, it is worth emphasizing that aside from the size dependent Young's modulus, we have not employed any surface elastic-type continuum theories[29,30] to compare the MD results. Rather, all the nanowires (beams) have been treated as homogeneous continua where the only size effect comes from the size dependent Young's modulus from Table I.

Finally, we note that the increased importance of shearing and rotary inertia has nothing to do with the fact that the nanowires are subject to nanoscale surface effects such as surface stresses as compared to macroscopic beams. Instead, it is an effect that stems from the aspect ratio as it is well known that the importance of these quantities decrease with increasing slenderness, as we recall that the nanowires we have considered so far have aspect ratios close to 12.

B. Pure modes

The mixed mode simulations have implied that the amount of shearing increases for higher modes. To study this closer we did study the dynamics of nanowires which are initially loaded such that they are excited by almost pure modes or with one dominating mode. During the simulations we took snapshots to monitor the rotation (ψ) and deflective (dw/dx) angles along the wire axis. The angle ψ is calculated by making least-squares approximations of the rotation angles of the individual vertical atomic planes. The angle, dw/dx, is obtained by finding the centers of mass for each vertical atomic plane and then calculating the angle using a finite difference scheme, as in Ref. 37. This approach enables us to study how the nanowires actually deform, to determine the amount of shearing, and to finally analyze if the hypothesis that the amount of shearing increases with higher modes is true.

In Fig. 4(a), we show the deflection of the center line of a nanowire at the time of the snapshot. The nanowire was excited so that it follows the mode shape of the fundamental mode quite closely, which it shows a clear resemblance to. In Fig. 4(b) a comparison between the deflective and rotation angles is given along the wire axis and it can be seen that the two curves follow each other very closely. The magnitudes of the differences between the curves can be seen in Fig. 4(c) where it appears that there is some kind of boundary effect at the ends of the nanowires, where the amounts of shearing are found to be the greatest. But comparing the magnitudes of differences in Fig. 4(c) with the magnitudes of the angles in Fig. 4(b) it is found that the relative amounts of shearing are quite small in comparison.

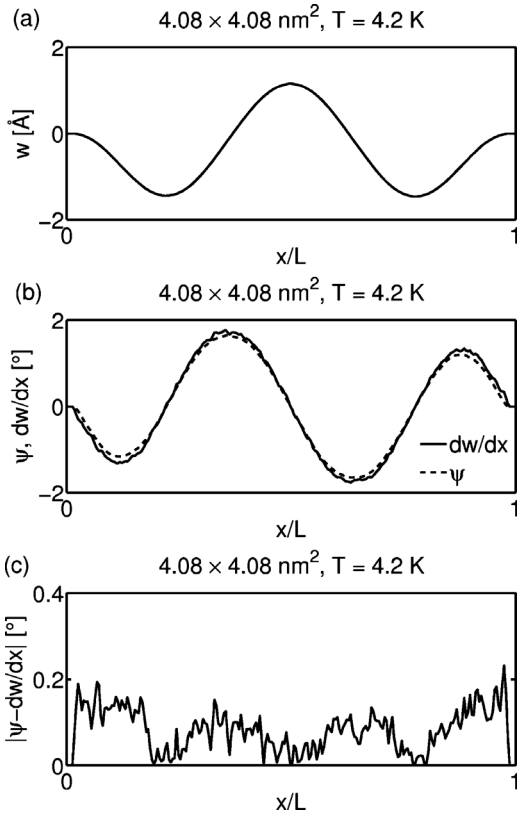

FIG. 6. Snapshot of the nanowire when the second excited mode is the dominating exciting mode. (a) Deflective shape of the center line for the snapshot, (b) the deflective angle of the center line and the rotation angle of the vertical atomic planes, and (c) the difference between the deflective angle and the rotation angle.

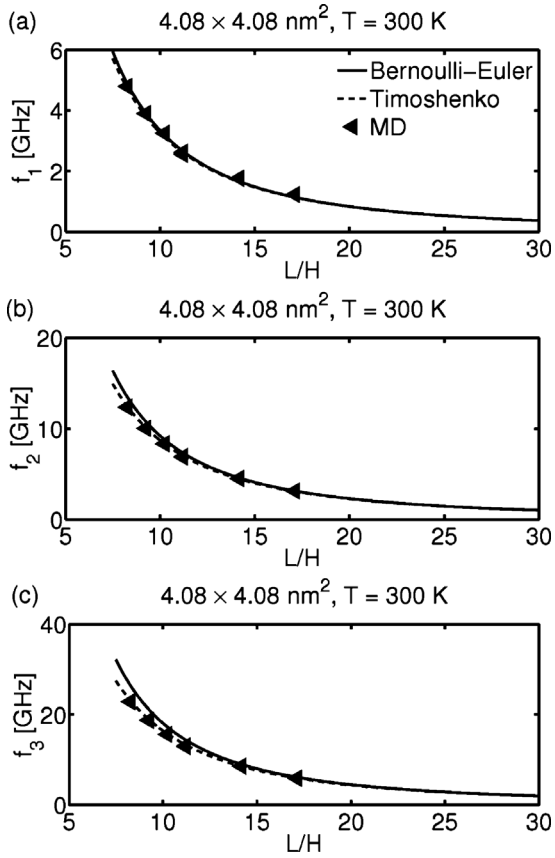

FIG. 7. Eigenfrequencies of (a) the fundamental, (b) first excited, and (c) second excited modes of unstressed nanowires for various aspect ratios.

In the same way, we have analyzed the pure mode behavior of the first and second excited modes, see Figs. 5 and 6, respectively. From Figs. 5(c) and 6(c) it is seen that the same kind of boundary effects arise also for the higher modes. Furthermore, it is observed that the magnitudes of shearing are of the same order as in Fig. 4(c), however, from Figs. 5(b) and 6(b) it is noted that the magnitudes of the angles decrease with increasing mode number. Moreover, it can be observed that the maximum amounts of shearing occurs at the inflection points. This implies that the relative amounts of shearing increases when we consider higher modes, as the number of inflection points increase with higher modes. This is in agreement with the results from the mixed mode simulations.

C. Aspect ratios

Finally, we have studied how the three lowest eigenfrequencies vary for unstressed nanowires of different aspect ratios. From Fig. 7 it can be concluded that, just like for the previously presented results, the MD results for the fundamental mode is in good agreement with both the Timoshenko and Bernoulli–Euler beam theories for essentially all the considered aspect ratios. Moreover, for the first and second excited modes it is seen that the Timoshenko predictions are in better agreement with the MD results than the Bernoulli–Euler continuum model. However, for all the considered modes one can clearly see that there is a converging trend, and when the aspect ratio is around 15–20 the different continuum models predict essentially the same results. Hence, it appears that the reason why the excited modes are not in that good agreement with the Bernoulli-Euler beam theory is merely lack of shearing and rotary inertia in the model, which is rooted in the fact that an aspect ratio of 12 is not sufficient in order for the shearing and rotary inertia to be negligible for higher modes. Therefore, the reason for the discrepancies is merely a geometric effect and has very little to do with the fact that surfaces deform the most under transverse loading or that it is a nanostructure. This means that, we are able to describe the eigenfrequency spectrum of both unstressed and prestressed nanowires very accurately using a simple continuum model and a nonlinear elastic constitutive relation which relates the stress to the strain.

Experimentally, the aspect ratios are often higher than the 15–20,[10,12,15–17,24] which we have considered here. This means that, in many practical applications this problem will not arise due to the geometry. However, for macroscopic thin-walled structures it is well known that contributions of rotary inertia and shearing becomes increasingly important.[38] Thus, it is likely that these contributions must be taken into account when nanotubes are considered. Furthermore, it is certainly an issue in numerical simulations; this is because in using MD, it is not feasible to perform simulations of nanowires that are much larger than has been considered here, for two reasons. First, as larger nanowires and thus more atoms are considered, the heavier the numerical effort becomes, though this can be mitigated using parallel computing. Sec-

ond, and more importantly, for the mechanical energy to be preserved in a conservative system and to accurately resolve the thermal vibrations, the timestep must be on the order of 1 fs in MD simulations. Thus, it requires on the order of 10^6 time increments to simulate 1 ns, which is problematic because it implies that the eigenfrequencies of the nanowires must be of the order of gigahertz if it is going to be practical to simulate them using MD. This puts geometric constraints on the aspect ratio, as the stiffness decreases with increasing aspect ratio.

V. SUMMARY AND CONCLUSIONS

In this paper, we have studied the resonant properties of unstressed and prestressed nanowires through MD simulations. For comparison, two different continuum mechanical beam models were used to describe the eigenfrequency spectrum; Bernoulli–Euler and Timoshenko beam theories. When studying prestressed nanowires, a size dependent nonlinear stress versus strain relation fitted to results from tensile simulations was used to describe the axial stresses.

We have demonstrated the increasing discrepancy between Bernoulli–Euler beam theory and MD results for higher modes and a consistent agreement between MD results and Timoshenko beam theory for all the considered modes. The underlying reason for these discrepancies is mainly geometric and it comes from the fact that the considered nanowires have a quite small aspect ratio. Even though both the Bernoulli–Euler and Timoshenko models describe the fundamental mode accurately, the relative amount of shearing as well as the contribution to the kinetic energy of the rotary inertia increases with increasing modes, as higher order mode shapes have more inflection points than lower order mode shapes and higher eigenfrequencies. This means that shearing and rotary inertia become increasingly important for higher modes and thus Bernoulli–Euler beam theory fails to describe the eigenfrequencies of the higher modes. Different aspect ratios were tested to see whether any convergence between Bernoulli–Euler and Timoshenko beam theories could be found, and this was found when the nanowire aspect ratios were roughly between 15–20.

Finally, we emphasize that apart from employing a nonlinear size dependent relation between the stress and the strain, we did not make any other assumptions about any surface or size effects. This means that we have treated the nanowires as homogeneous beams and have therefore not made any additional assumptions to account for the different elastic properties of nanoscale surfaces. Despite this, we have managed to get good agreement between MD results and Timoshenko beam theory, even for higher order resonant frequencies where surface effects are expected to have a greater effect.

ACKNOWLEDGMENTS

P.A.T.O. gratefully acknowledges the funding provided by the Swedish research council. H.S.P. gratefully acknowledges the support of NSF under Grant No. 0856261. The simulations were performed using the computational resources at LUNARC, Center for Scientific and Technical Computing, Lund University.

[1] H. G. Craighead, Science **290**, 1532 (2000).
[2] K. L. Ekinci and M. L. Roukes, Rev. Sci. Instrum. **76**, 061101 (2005).
[3] K. L. Ekinci, X. M. H. Huang, and M. L. Roukes, Appl. Phys. Lett. **84**, 4469 (2004).
[4] Y. T. Yang, C. Callegari, X. L. Feng, K. L. Ekinci, and M. L. Roukes, Nano Lett. **6**, 583 (2006).
[5] L. G. Zhou and H. Huang, Appl. Phys. Lett. **84**, 1940 (2004).
[6] H. Liang, M. Upmanyu, and H. Huang, Phys. Rev. B **71**, 241403(R) (2005).
[7] H. S. Park, W. Cai, H. D. Espinosa, and H. Huang, MRS Bull. **34**, 178 (2009).
[8] R. Dingreville, J. Qu, and M. Cherkaoui, J. Mech. Phys. Solids **53**, 1827 (2005).
[9] M. T. McDowell, A. M. Leach, and K. Gall, Modell. Simul. Mater. Sci. Eng. **16**, 045003 (2008).
[10] A. Gupta, D. Akin, and R. Bashir, Appl. Phys. Lett. **84**, 1976 (2004).
[11] M. B. Viani, T. E. Schäffer, A. Chand, M. Reif, H. E. Gaub, and P. K. Hansma, J. Appl. Phys. **86**, 2258 (1999).
[12] B. Ilic, D. Czaplewski, H. G. Craighead, P. Neuzil, C. Campagnolo, and C. Batt, Appl. Phys. Lett. **77**, 450 (2000).
[13] T. D. Stowe, K. Yasumura, T. W. Kenny, D. Botkin, K. Wago, and D. Rugar, Appl. Phys. Lett. **71**, 288 (1997).
[14] H. Petrova, J. Perez-Juste, Z. Zhang, J. Zhang, T. Kosel, and G. V. Hartland, J. Mater. Chem. **16**, 3957 (2006).
[15] M. Lexholm, I. Karlsson, F. Boxberg, and D. Hessman, Appl. Phys. Lett. **95**, 113103 (2009).
[16] A. Husain, J. Hone, H. W. Ch. Postma, X. M. H. Huang, T. Drake, M. Barbic, A. Scherer, and M. L. Roukes, Appl. Phys. Lett. **83**, 1240 (2003).
[17] V. Cimalla, Ch. Foerster, F. Will, K. Tonisch, K. Brueckner, R. Stephan, M. E. Hein, O. Ambacher, and E. Aperathitis, Appl. Phys. Lett. **88**, 253501 (2006).
[18] S. S. Verbridge, J. M. Parpia, R. B. Reichenbach, L. M. Bellan, and H. G. Craighead, J. Appl. Phys. **99**, 124304 (2006).
[19] S. S. Verbridge, D. Finkelstein Shapiro, H. G. Craighead, and J. M. Parpia, Nano Lett. **7**, 1728 (2007).
[20] B. Wu, A. Heidelberg, and J. J. Boland, Nature Mater. **4**, 525 (2005).
[21] A. Heidelberg, L. T. Ngo, B. Wu, M. A. Phillips, S. Sharma, T. I. Kamins, J. E. Sader, and J. J. Boland, Nano Lett. **6**, 1101 (2006).
[22] S. Cuenot, C. Frétigny, S. Demoustier-Champagne, and B. Nysten, Phys. Rev. B **69**, 165410 (2004).
[23] G. Y. Jing, H. L. Duan, X. M. Sun, Z. S. Zhang, J. Xu, Y. D. Li, J. X. Wang, and D. P. Yu, Phys. Rev. B **73**, 235409 (2006).
[24] S. G. Nilsson, E. L. Sarwe, and L. Montelius, Appl. Phys. Lett. **83**, 990 (2003).
[25] S. G. Nilsson, X. Borrisé, and L. Montelius, Appl. Phys. Lett. **85**, 3555 (2004).
[26] N. V. Lavrik, M. J. Sepaniak, and P. G. Datskos, Rev. Sci. Instrum. **75**, 2229 (2004).
[27] H. S. Park, P. A. Klein, and G. J. Wagner, Int. J. Numer. Methods Eng. **68**, 1072 (2006).
[28] H. S. Park and P. A. Klein, Phys. Rev. B **75**, 085408 (2007).
[29] J. He and C. M. Lilley, Appl. Phys. Lett. **93**, 263108 (2008).
[30] J. He and C. M. Lilley, Nano Lett. **8**, 1798 (2008).
[31] H. S. Park, J. Appl. Phys. **104**, 013516 (2008).
[32] H. S. Park and P. A. Klein, J. Mech. Phys. Solids **56**, 3144 (2008).
[33] H. S. Park, J. Appl. Phys. **103**, 123504 (2008).
[34] J. Q. Broughton, C. A. Meli, P. Vashishta, and R. K. Kalia, Phys. Rev. B **56**, 611 (1997).
[35] G. Cao, X. Chen, and J. W. Kysar, Phys. Rev. B **72**, 195412 (2005).
[36] P. A. T. Olsson, J. Appl. Phys. **108**, 034318 (2010).
[37] P. A. T. Olsson, S. Melin, and C. Persson, Phys. Rev. B **76**, 224112 (2007).
[38] M. Géradin and D. Rixen, *Mechanical Vibrations: Theory and Application to Structural Dynamics*, 2nd ed. (Wiley, New York, 1997).
[39] See supplementary material at http://dx.doi.org/10.1063/1.3460127 to Ref. 36 for the derivation of the secular equation of Eq. (1) and the parametrization of the EAM potential.
[40] S. Timoshenko, D. H. Young, and W. Weaver, Jr., *Vibration Problems in Engineering*, 4th ed. (Wiley, New York, 1974).
[41] C. T. Sun, Trans. ASME, J. Appl. Mech. **39**, 282 (1972).